

IDENTIFICATION OF DYNAMIC RIGIDITY FOR HIGH SPEED SPINDLES SUPPORTED ON BALL BEARINGS

Jakeer Hussain Shaik¹, Srinivas J²

¹Research Scholar, ²Associate Professor, Department of Mechanical Engineering, National Institute of Technology, Rourkela, Odisha, India, jakeershaik786@yahoo.co.in

Abstract

The widespread use of high-speed machining in recent decades has led to a significant area of research on issues that limit its productivity. Regenerative chatter is a well-known machining problem that results in unstable cutting process, leads to the poor surface quality, reduced material removal rate and damage on the machine tool itself. The main requirement for the stability of system dynamics is the information of tool tip frequency response functions (FRF's). The present work considered a coupled model of spindle-bearing system by using the angular contact ball bearing forces on stability of machining. Using Timoshenko beam element formulation, the spindle unit is analyzed by including the gyroscopic and centrifugal terms and the bearing contact forces are arrived from Hertzian contact theory. Then, the model is used for studying the effects of viscous damping to obtain the tool point FRF for the dynamic spindle.

Index Terms: Spindle dynamics, Stability, High speed effects, Bearing contact forces, Hertzian contact theory, Finite element modeling.

1. INTRODUCTION

In recent years there has been keen interest by manufacturers to increase Productivity and Surface quality of part by using High speed milling machines. This has direct impact on cost of machining and Quality. Dynamic rigidity is one of the most critical characteristics of machine tools, especially for high precision and high performance machining applications. This technology is mainly limited by the performance of the spindle which has a significant influence on the machining accuracy. Self-excited vibrations of the tool result in unstable cutting process which leads to the chatter on the work surface and it reduces the productivity. At large rates of material removal, tool chatter creates the unavoidable flexibility between the cutting tool and the work piece; if it is uncontrolled the chatter causes a rough surface finish and dimensional inaccuracy of the work piece along with unacceptable loud noise levels and accelerated tool wear. The chatter stability of the tool is dependent on the dynamic behavior of the spindle system, which is often expressed as the frequency response function (FRF) at the tool tip. In other words, tool-tip FRF is a key variable in determination of stability limit [1]. The objective of the design engineer is to predict the cutting performances of the spindle during the design stage by relying on engineering model of the process and system dynamics. Early spindle research has focused mainly on static analysis, where as current research is extended to the dynamics for optimal design.

Over the last two decades, numerous approaches have been addressed to elaborate the tool-tip FRF through modeling and experiments. With introduction of receptance coupling substructure analysis by Schmitz in early 2000, several authors [2-7] have illustrated the approach to predict the tool point FRFs. Erturk et al.[8] presented analytical models to obtain the tool-tip FRF. Faassen et al. [9] predicted chatter stability lobes of high speed milling on the basis of experimental FRFs at different spindle speeds. Abele and Fiedler [10] introduced a sub-space-state-space-identification method to measure and calculate the dynamic behavior of spindle-tool systems during high speed machining, consequently, stability lobe diagrams were determined based on the identified FRFs. Zaghbani and Songmene [11] used operational modal analysis to estimate the machine tool dynamic parameters during high machining operations, and the dynamic stability lobes were calculated using the extracted modal parameters. The experimental method is used to identify speed-varying dynamics of spindles in the above works, which is direct and feasible. However, it is time-consuming to repeat the modal tests for every spindle speed and prone to errors. With known details of the spindle geometry, drawbar force, bearing parameters and preload, etc., an alternative method to obtain the dynamic behavior of spindle system is the finite element (FE) method. With the accurate spindle model, the FRFs at the tool tip are simulated and then chatter stability lobes can be predicted. Chen and Wang [12] modeled the integrated spindle-bearing system and they also found that significant errors occurred in predicting stability lobes if the load and speed effects on the

shaft/bearing dynamics were neglected. Tian and Hutton [13] considered the gyroscopic effects of the rotating spindle and proposed a chatter model in milling systems. They found that gyroscopic effects reduced the critical axial depth of cut. Similarly, Movahhedy and Mosaddegh [14] predicted the chatter in high speed milling including gyroscopic effects on the basis of FE spindle model. Gagnol et al. [15] developed a dynamic model of a high-speed spindle system and then proposed a dynamic stability lobe diagram by integrating the speed-dependent FRFs of spindles into analytical approach of Altintas and Budak [16]. Angular contact ball bearings are commonly used in high-speed spindles due to their low-friction properties and ability to withstand external loads in both radial and axial directions. Although the ball bearings appear to be a simple mechanism, their internal geometry is quite complex and often display very complicated nonlinear dynamic behavior. It is obvious that the spindle machining system supported by ball bearings present interesting stability characteristics and nonlinear responses. Several recent studies [17-21] illustrated the dynamics of high speed spindles under different preload mechanisms and operating speeds.

Present paper describes a coupled model of spindle-bearing system by considering the effects of ball bearing Hertz contact forces on the spindle dynamics. The governing differential equations of motion of spindle system are employed and numerical simulations are carried-out using Timoshenko beam element model.

2. MODELING OF SPINDLE-BEARING SYSTEM

The spindle system generally consists of spindle housing carrying spindle shaft over the front and rear bearings, a tool holder and tool as shown in Fig.1.



Fig-1: Schematic of end-mill spindle unit

The dynamic behavior of the spindle-tool unit can be well established through the modeling of the restricted spindle rotating system as shown in Fig.2. The spindle has six elements, seven nodes and total 28 degrees of freedom. Both the fifth and seventh nodes of the shaft are supported by two

angular contact bearings. The x and y directional cutting forces act on the tool tip. Tool is assumed to be rigidly connected to the tool holder which is fixed to the spindle shaft.

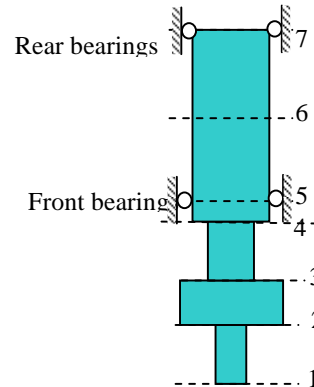


Fig-2: Equivalent analysis model

The equations of motion for the spindle shaft due to rotation are given by [22-23]:

$$\rho A \frac{d^2 v}{dt^2} - \frac{\partial}{\partial x} \left[k_s AG \left(\frac{\partial v}{\partial x} - \theta_z \right) - P \frac{\partial v}{\partial x} \right] - \Omega^2 \rho A v = F_x \quad (1)$$

$$\rho A \frac{d^2 w}{dt^2} - \frac{\partial}{\partial x} \left[k_s AG \left(\frac{\partial w}{\partial x} + \theta_y \right) - P \frac{\partial w}{\partial x} \right] - \Omega^2 \rho A w = F_y \quad (2)$$

$$\rho I \frac{d^2 \theta_y}{dt^2} + \Omega \rho J \frac{d \theta_z}{dt} - EI \frac{\partial^2 \theta_y}{\partial x^2} + k_s AG \left(\frac{\partial w}{\partial x} + \theta_y \right) = M_x \quad (3)$$

$$\rho I \frac{d^2 \theta_z}{dt^2} - \Omega \rho J \frac{d \theta_y}{dt} - EI \frac{\partial^2 \theta_z}{\partial x^2} - k_s AG \left(\frac{\partial v}{\partial x} - \theta_z \right) = M_y \quad (4)$$

Here, v and w are the bending deformation in two perpendicular directions of the spindle unit. ρA is mass per unit length of spindle shaft, ks is shear deformation factor, EI is flexural rigidity, AG is shear rigidity of the shaft material, ρJ is polar modulus, Fx and Fy are the components of external forces, Mx and My are the components of transverse moments and Ω is the speed of rotation of spindle shaft.

A rotating shaft with eight degrees of freedom per node finite beam element with gyroscopic terms based on Timoshenko beam theory formulated by Nelson [24] is employed to model the rotating spindle. The element translational and rotational mass matrices, the stiffness matrix and gyroscopic matrix are

obtained by applying Hamilton's principle. The governing equation in matrix form obtained using FE method is:

$$[M]\{\ddot{q}\} + [C]\{\dot{q}\} + ([K] - \Omega^2[M_c])\{q\} = F \tag{5}$$

Where the system element matrices are given by [18]:

$$[M] = [MT] + [MR] \tag{6}$$

$$[MT] = [M0] + \phi[M1] + \phi^2[M2] \tag{7}$$

$$[MR] = [N0] + \phi[N1] + \phi^2[N2] \tag{8}$$

$$[K] = [K0] + \phi[K1] \tag{9}$$

$$[C] = -\Omega[G] + \alpha[M] + \beta[K] \tag{10}$$

$$\phi = \frac{12EI}{k_s AGl^2} \tag{11}$$

The front and rear positions of the spindle shaft are supported by the similar angular contact ball bearings. Without considering the axial forces and moment loadings of the spindle system, the angular contact ball bearings can be assumed as deep-groove ball bearings and the dynamic problem of the angular contact ball bearing is made as one of the two degrees of freedom. The local Hertz contact forces and deflection relationships for a ball with the inner and outer races may be written as a following set of restoring forces:

$$F_{X1} = -c_{b1}\dot{x}_{b1} - \sum_{i=1}^{N_b} k_{b1}(x_{b1} \cos \phi_i + y_{b1} \sin \phi_i - \delta)^{1.5} \cos \phi_i \tag{12}$$

$$F_{Y1} = -c_{b1}\dot{y}_{b1} - \sum_{i=1}^{N_b} k_{b1}(x_{b1} \cos \phi_i + y_{b1} \sin \phi_i - \delta)^{1.5} \sin \phi_i \tag{13}$$

$$F_{X2} = -c_{b2}\dot{x}_{b2} - \sum_{i=1}^{N_b} k_{b2}(x_{b2} \cos \phi_i + y_{b2} \sin \phi_i - \delta)^{1.5} \cos \phi_i \tag{14}$$

$$F_{Y2} = -c_{b2}\dot{y}_{b2} - \sum_{i=1}^{N_b} k_{b2}(x_{b2} \cos \phi_i + y_{b2} \sin \phi_i - \delta)^{1.5} \sin \phi_i \tag{15}$$

Here δ refers to the initial clearance of the bearings, N_b is number of balls, x_{b1} and y_{b1} , x_{b2} and y_{b2} are the displacements of mass elements distributed at the front and rear bearing nodes along x and y directions respectively, k_{b1} and c_{b1} , k_{b2} and c_{b2} are the stiffness and damping of front and rear bearings respectively, and the

$$\phi_i = \left[\frac{\Omega r}{(R+r)} \right] t + \left(\frac{2\pi}{N_b} \right) (i-1) \tag{16}$$

angle (where $i=1,2,\dots,N_b$) is the angular location of the i th ball. Here the term: $x_{b1}\cos\phi_i + y_{b1}\sin\phi_i - \delta$ is accounted only when it is positive, otherwise it is taken as zero and the bearing races are at loss of contact with bearing balls. An idealized condition is considered in present work with $\delta = -0.05 \mu\text{m}$ (considering practical conditions, the interference fit generally adopted to chatter problems where negative clearance is justified) and negligible value of bearing damping, inner radius $r=40 \text{ mm}$, outer radius $R=60\text{mm}$, number of ball $N_b=8$, $k_{b1}=k_{b2}=13.34 \times 10^9 \text{ N/m}^{3/2}$. The spindle FRF consisting of real and imaginary parts can be given expressed as:

$$[H(j\omega)] = [\text{Re}(\omega)] + j[\text{Im}(\omega)] = [-[M]\omega^2 + j\omega[C] + ([K] - \Omega^2[M_c])]^{-1} \tag{16}$$

Here, Re and Im are, respectively, the real and imaginary part of the transfer function of the spindle tool tip.

3. RESULTS

The parameters of the finite element model of the spindle are illustrated in Table 1. Except the element-1 (Silicon carbide tool) and all other elements are taken as steel. Densities and shear modulus are considered for the problem is obtained from tables.

Table -1: Parameters for finite element model of the spindle [18].

Parameter	Elements of the spindle					
	1	2	3	4	5	6
Length(mm)	45	40	50	20	200	20
Outer dia.(mm)	19	74.5	40	60	60	60
Inner dia.(mm)	0	0	0	0	40	40
E (GPa)	450	210	210	210	210	210
Parameter	45	40	50	20	200	20

Computer program is developed in MATLAB to analyze the spindle system. The assembly matrices and static condensation approach to eliminate the rotational degrees of freedom are included in the program. Initially, by assuming the bearings to be perfectly rigid, Campbell diagram is obtained as shown in Fig.3. Using undamped natural frequencies, the coefficients of Rayleigh's damping α and β are obtained as 17.32 and 3.87×10^{-6} respectively for 1% damping ratio.

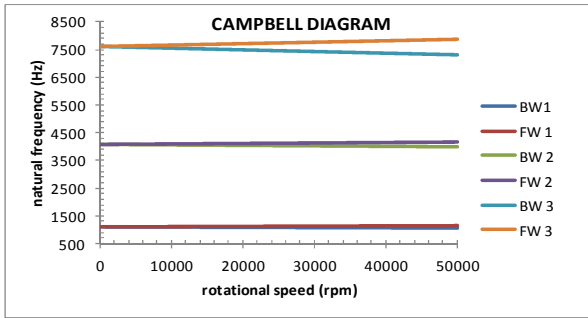


Fig-3: First three natural frequencies of spindle rotor

Here the viscous damping forces and centrifugal stiffening are not accounted. The forward and backward whirl modes are obvious due to the gyroscopic effect at three first natural frequencies 1098.8 Hz, 4079.1 Hz and 7590.57 Hz respectively. In order illustrate the centrifugal stiffening effect and bearing dynamics, direct frequency response function at the tool tip $h_{xx}(j\omega)$ is illustrated at different spindle speeds (Ω). Fig.4. depicts the FRF without considering Rayleigh’s damping for the spindle mounted on rigid bearings at two different speeds. The effect of centrifugal stiffening is observed at higher speeds only as seen in Fig.5.

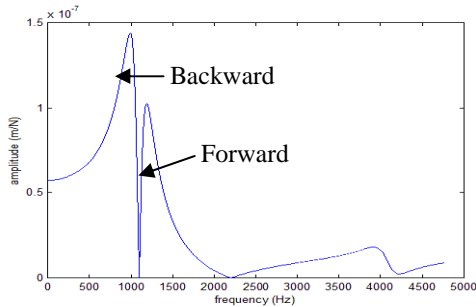


Fig-4: Frequency response at 7000 rpm

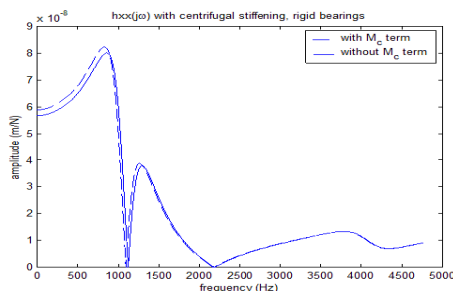


Fig-5: Frequency response at 15000 rpm

Unlike direct FRF, the cross FRF is a smooth curve without showing backward (BW) and forward (FW) whirl modes as seen from the Fig.6. obtained at 15000 rpm.

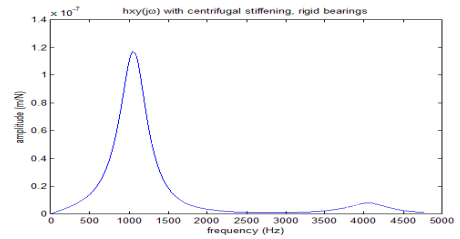


Fig-6: Cross frequency response at 15000 rpm

The effect of Rayleigh’s (viscous) damping on the tool tip FRF is shown at 12000 rpm as shown in Fig.7. It is seen that damping affects considerably the whirl modes.

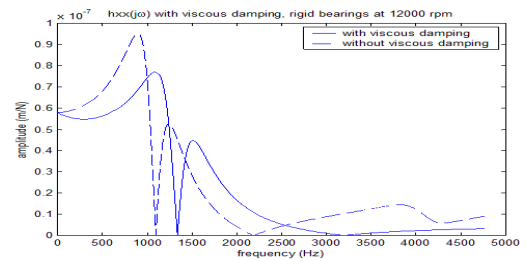


Fig-7: Effect of viscous damping at a speed 12000 rpm

For studying the bearing effect, the solution is obtained as a transient analysis problem first in time domain and then the frequency spectrum is obtained from fast Fourier transformation (FFT) algorithm. The reduced coupled differential equations (14 in number) were solved by explicit Runge Kutta solver time integration schmes. Fig.8. and Fig.9. shows the time histories and FFT diagram at the tool-tip node.

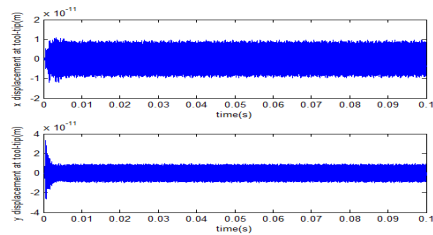


Fig-8: Time histories

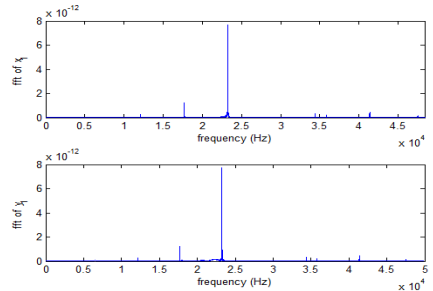


Fig-9: Frequency responses

It has been observed clearly from the frequency responses that the natural frequencies of the spindle have been affected by the bearing contact forces.

CONCLUSIONS

In this work a coupled model of spindle bearing system is considered for illustration and it was analyzed using finite element analysis by considering the effect of shear deformation and rotary inertia of spindle shaft. It was observed that the Centrifugal and gyroscopic forces on the spindle rotor affect respectively the stiffness and damping of the system. The viscous damping was also accounted and the bearings were treated first as a rigid supports. Bearing forces expressed as functions of corresponding nodal displacements using Hertz contact theory have also been included in the final model in order to investigate effect of the angular contact bearings. The resulting FRF obtained by the spindle bearing model can be used in the existing analytical and numerical models for constructing the accurate stability lobe diagrams for the high speed machining process.

REFERENCES

- [1]. Altintas and E. Budak, 1995: Analytical prediction of stability lobes in milling. *Annals of the CIRP*. **44**, 357–362.
- [2]. T.L. Schmitz, M.A. Davies, K. Medicus and J. Snyder, 2001: Improving high-speed machining material removal rates by rapid dynamic analysis. *Annals of the CIRP*. **50**, 263–268.
- [3]. T.L. Schmitz, J.C. Ziegert and C. Stanislaus, 2004: A method for predicting chatter stability for systems with speed-dependent spindle dynamics. *Trans. North Amer. Manuf. Res. Institution of SME*. **32**, 17–24.
- [4]. T.L. Schmitz and G.S. Duncan, 2005: Three-component receptance coupling substructure analysis for tool point dynamics prediction. *J Manuf Sci Eng*. **127**, 781–791.
- [5]. C.H. Cheng, T.L. Schmitz and G.S. Duncan, 2007: Rotating tool point frequency response prediction using RCSA. *Machining Science and Technology*. **11**, 433–446.
- [6]. Z.Jun, S.Tony, Z.Wanhua and L.U.Bingheng, 2011: Receptance coupling for tool point dynamics prediction on machine tools. *Chinese J.Mech.Engg*. **24**, 1-6.
- [7]. U.V.Kumar and T.L.Schmitz, 2012: Spindle dynamics identification for Receptance Coupling Substructure Analysis. *Precision Engineering*. **36**, 435– 443.
- [8]. A.Erturk, E.Budak and H.N.Ozguven, 2007: Selection of design and operational parameters in spindle-holder-tool assemblies for maximum chatter stability by using a new analytical model. *Int. J. Machine Tools & Manf*. **47**, 1401–1409.
- [9]. R.P.H. Faassen, N. V.Wouw, J.A.J. Oosterling and H. Nijmeijer, 2003: Prediction of regenerative chatter by modelling and analysis of high-speed milling. *Int. J. Machine Tools & Manf*. **43**, 1437–1446.
- [10]. E. Abele and U. Fiedler, 2004: Creating stability lobe diagrams during milling. *Annals of the CIRP*. **53**, 309–312.
- [11]. Zaghbani and V. Songmene, 2009: Estimation of machine-tool dynamic parameters during machining operation through operational modal analysis. *Int. J. Machine Tools & Manuf*. **49**, 947–957.
- [12]. C.H. Chen and K.W. Wang, 1994: An integrated approach toward the dynamic analysis of high-speed spindles. 2. Dynamics under moving end load. *J. Vibration and Acous.*, *Trans.ASME*. **116**, 514–522.
- [13]. J.F. Tian and S.G. Hutton, 2001: Chatter instability in milling systems with flexible rotating spindles—a new theoretical approach. *J.Manuf. Sci. and Engg. Trans.ASME*. **123**, 1–9.
- [14]. M.R. Movahhedy and P. Mosaddegh, 2006: Prediction of chatter in high speed milling including gyroscopic effects. *Int. J. Machine Tools & Manuf*. **46**, 996–1001.
- [15]. V.Gagnol, B.C. Bougarrou, P. Ray and C. Barra, 2007: Stability based spindle design optimization. *J. Man. Sci. Eng. Trans. ASME*. **129**, 407-415.
- [16]. Y. Altintas and E. Budak, 1995: Analysis prediction of stability lobes in milling. *Annals of CIRP*. **44**, 357–362.
- [17]. S. Jiang and S.Zheng, 2010: A modeling approach for analysis and improvement of spindle-drawbar-bearing assembly dynamics. *Int. J.Mach. Tools & Manuf*. **50**, 131–142.
- [18]. S.H.Gao, G.Meng and X.H.Long, 2010: Stability prediction in high-speed milling including the thermal preload effects of bearing. *J.Process Mech.Engg.*, *Proc.IMechE*. **224**, 11-22.
- [19]. H.Cao, T.Holkup and Y.Altintas, 2011: A comparative study on the dynamics of high speed spindles with respect to different preload mechanisms. *Int J Adv Manuf Technol*. **57**, 871-883.
- [20]. V.Gagnol, T.P. Le and P. Ray, 2011: Modal identification of spindle-tool unit in high-speed machining. *Mech. Sys.Sig.Proc*. **25**, 2388–239.
- [21]. H.Cao, B.Li and Z.He, 2012: Chatter stability of milling with speed-varying dynamics of spindles. *Int.J.Mach.Tools and Manuf*. **52**, 50-58.
- [22]. Y.Cao and Y.Altintas, 2004: A general method for modeling of spindle bearing system. *J.Mech.Design, Trans.ASME*. **126**, 1089-1104.
- [23]. M.Rantatalo, J.O.Aidanpaa, B.Goransson and P.Norman, 2007: Milling machine spindle analysis using FEM and non-contact spindle excitation and response measurement. *Int. J. Machine Tools & Manuf*. **47**, 1034-1045.
- [24]. H.D Nelson, 1980: A finite rotating shaft element using Timoshenko beam theory. *J.of machine design*. **102**:793-803.